ELSEVIER

Journal of Power Sources 101 (2001) 219–225

JOURNAL OF POWER SOURCES

www.elsevier.com/locate/jpowsour

Physical and electrochemical characterization of PbO_2 electrode prepared at different $H_2SO_4/H_2O/PbO$ ratios

Chih-Hsuan Yeh[a], Chi-Chao Wan[a], Jenn-Shing Chen[b,*]

[a]*Department of Chemical Engineering, Tsing-hua University, Hsin-Chu 300, Taiwan, ROC*
[b]*Department of Chemical Engineering, I-Shou University, Ta-Hsu Hsiang, Kaohsiung County 840, Taiwan, ROC*

Received 1 December 2000; accepted 31 January 2001

Abstract

The influence of pastes from various $H_2SO_4/H_2O/PbO$ ratios on the material structure and electrochemical characteristics of PbO_2 electrodes is studied. The structural and electrochemical characteristics of these electrodes are investigated by scanning electron microscopy (SEM), X-ray diffraction, mercury intrusion porosimetry (MIP), ac impedance, and charge–discharge curves. Three pastes (A, B, and C) are studied to assess the influence of $H_2SO_4/H_2O/PbO$ ratios. Paste A, prepared with more water, has a larger specific surface-area and pore-size. The group A plates have a greater porosity, which gives higher active material utilization and higher initial capacity. The plates have poor mechanical strength, however, which results in a high capacity loss for each cycle. In studies on ac impedance, the appearance of a high-frequency inductive loop in the group A plates indicates that these plates have active materials of greater porosity during the electrode processing reactions. The group C plates, prepared with more H_2SO_4, contained more α-PbO_2 crystals which results in a smaller charge-transfer resistance, and a larger exchange current.

Keywords: Valve-regulated lead/acid cell; Lead dioxide electrode; Paste; Charge-transfer resistance

1. Introduction

Paste preparation is a key step in the production of active materials that determine the design life and performance characteristics of lead-acid batteries. In addition, the paste must flow under pressure into the lattice framework of the grid and must be retained there throughout the subsequent curing and drying process in which the material acquires its rigidity and particle-to-particle cementation. Therefore, the main objectives in paste formulation and mixing should be

1. to provide good plastic-flow properties;
2. to retain sufficient moisture for effective curing;
3. to restrict shrinkage, sinkage and cracking;
4. to produce consistent density.

In addition, paste mixes are formulated to take into account many parameters, such as

1. starting oxide properties;
2. amounts of H_2SO_4 and H_2O;
3. mixing sequence;
4. mixing mechanics;
5. temperature;
6. time.

In this work, the effect of amounts of H_2SO_4 and H_2O on the paste properties has been examined. During paste mixing, a significant proportion of the total leady oxide is converted into one of three possible basic lead sulfates, namely, monobasic, $PbO{\cdot}PbSO_4$ (1BS), tribasic, $3PbO{\cdot}PbSO_4{\cdot}H_2O$ (3BS), or tetrabasic, $4PbO{\cdot}PbSO_4$ (4BS) [1]. These compounds serve to consolidate the paste through the development of interlocking crystalline networks. Generally, the dominance of a particular species, especially 3BS or 4BS, depends on the acid/oxide ratio, as well as the temperature and the mixing duration. As the 3BS and 4BS yield decreases, the 3BS size increases, and the 4BS size decreases, when using a low acid/oxide ratio [2]. Since the conversion of either 3BS or 4BS to PbO_2 is metasomatic, the PbO_2 is similar in size and the shape to its precursor. Therefore, the acid/oxide ratio is significant in controlling the phase composition and size of the 3BS and 4BS crystals and the characterization of PbO_2 crystals [1,2]. Also during mixing, the amounts of water and sulfuric acid are adjusted to ensure that the resultant wet paste has satisfactory plastic-flow properties and the wet-paste density is to specification.

* Corresponding author. Tel.: +886-7-657-8624; fax: +886-7-657-8945.
E-mail address: jschen@csas00.isu.edu.tw (J.-S. Chen).

0378-7753/01/$ – see front matter
PII: S0378-7753(01)00712-1

The paste density is almost a direct function of the total added fluids, especially the water. Since water is a much better bulking agent than sulfuric acid, the amount of sulfuric acid used has only a small effect on the wet-paste density and the important factor is the total water content.

The behavior of positive plates (PbO_2 electrodes) influences strongly the discharge service of the valve-regulated lead/acid battery (VRLA). The characterization of the positive plate is strongly dependent on the structure of the positive active material, which is influenced by the phase composition, crystal morphology and density of the initial paste [3–5]. In the production of positive plates, the paste composition is critical in obtaining an active material with preferred chemical species and optimum morphology/porosity. Therefore, in this work, a study was made of the effects of various H_2SO_4/H_2O/PbO ratios in positive pastes on the material structure and electrochemical characteristics of the plates. The structural and electrochemical characteristics of these electrodes have been investigated by scanning electron microscopy (SEM), X-ray diffraction, Brunauer–Emmet–Teller (BET-N_2) adsorption, mercury intrusion porosimetry (MIP), ac impedance, and charge–discharge tests.

2. Experimental procedures

2.1. Positive paste preparation and cell construction

The positive paste was prepared by mixing leady oxide with water, sulfuric acid, and fibre. Three positive paste compositions were examined (see Table 1). Mixing was continued for 35 min and the apparent density of the paste was about 3.9–4.1 g cm^{-3}. The paste was then applied to grids cast from a Pb–Ca alloy. The grid dimensions were 69 mm × 40 mm × 3.6 mm. The positive plates were controlled with around 33 g paste on each side of the grid and, then, cured. Curing was performed for 1 day at 50°C at a relative humidity of >90%. Prior to formation, the plates were dried in the air for 3–5 days until the moisture in the paste was <1 wt.%. The current density for formation was controlled at 6 mA cm^{-2} and the charge passed was about 200% of the theoretical capacity. After formation, the plates were washed in running water for several hours and then dried in an oven at 65°C for 24 h. All negative plates and absorptive glass-mat (AGM) separators were supplied by The Ztong Yee Battery Corporation (Taiwan). Each cell contained two positive plates and three negative plates. The cell was filled with 38 cm^3 of electrolyte and then sealed with a cover. In all experiments, each cell was filled with sulfuric acid solution, having a specific gravity of 1.335 (20°C). The cell's rated capacity was 4 Ah.

Table 1
Summary of different paste compositions with various H_2SO_4/H_2O/PbO ratios

Compound	Paste type		
	A	B	C
Leady oxide (kg)	5	5	5
H_2O (ml)	700	600	600
H_2SO_4 (specific gravity = 1.4 ml)	380	380	480

2.2. Cell cycling tests

Cells were cycled under computer-controlled charge and discharge regimens using an Arbin Battery Testing System. To render the cell active, all cells were charged at 0.23 A for 13 h before regular testing. The testing employed a discharge current of 0.8 A to a cut-off voltage of 1.75 V and a charge current of 0.4 A to 120% of the previous discharge capacity. In addition, an open-circuit period of 30 min was implemented at the end of each half-cycle. Cycling continued until the cell capacity dropped and remained below 80% of the initial capacity.

2.3. Analysis of positive-plate material

The physicochemical and electrochemical properties of the positive active-material, i.e. the phase composition,

Table 2
Comparison of phase composition and BET specific surface-area of paste, cured and formed materials and after 100 charge and discharge cycles of the active material

Compound	Type											
	Paste			After curing			After formation			After 100 cycles, and charged		
	A	B	C	A	B	C	A	B	C	A	B	C
Pb	4.8	5.4	6.9									
α-PbO	44.7	53	55.3	48.5	55.6	58.6						
β-PbO	7.1	4.2	2.5	4.7	2.5	3.1						
HC ($2PbCO_3 \cdot Pb(OH)_2$)	4.3	1.9	1.8	2.3	–	–						
3BS	39.1	35.5	33.5	44.5	41.9	38.3						
α-PbO_2							12.1	13.9	15.3	6.7	8.8	11.7
β-PbO_2							83.7	82	80.8	78.8	81.6	79.6
$PbSO_4$							4.2	4.1	3.9	14.5	9.6	8.7
BET specific surface area ($m^2\ g^{-1}$)	1.10	1.08	1.04	0.92	0.91	0.88	3.91	3.87	3.62			

morphology and pore-size, were obtained using X-ray powder diffraction (XRD), SEM, BET-N_2 adsorption, MIP, and ac impedance spectroscopy. All analytical samples taken from the pastes and plates were treated using the following steps [6]: (i) wash with distilled water (to remove acid); (ii) wash with absolute ethanol (to removed water) and dry in a desiccator; (iii) after drying, a portion of each sample was ground gently using a pestle and mortar.

3. Results and discussion

3.1. Analyses of plate composition and morphology

This work aims to determine the effects of various H_2SO_4/H_2O/PbO ratios on the material structure and electrochemical characteristics of the positive plates. Three pastes (see Table 1) A, B, C have been studied to assess these effects.

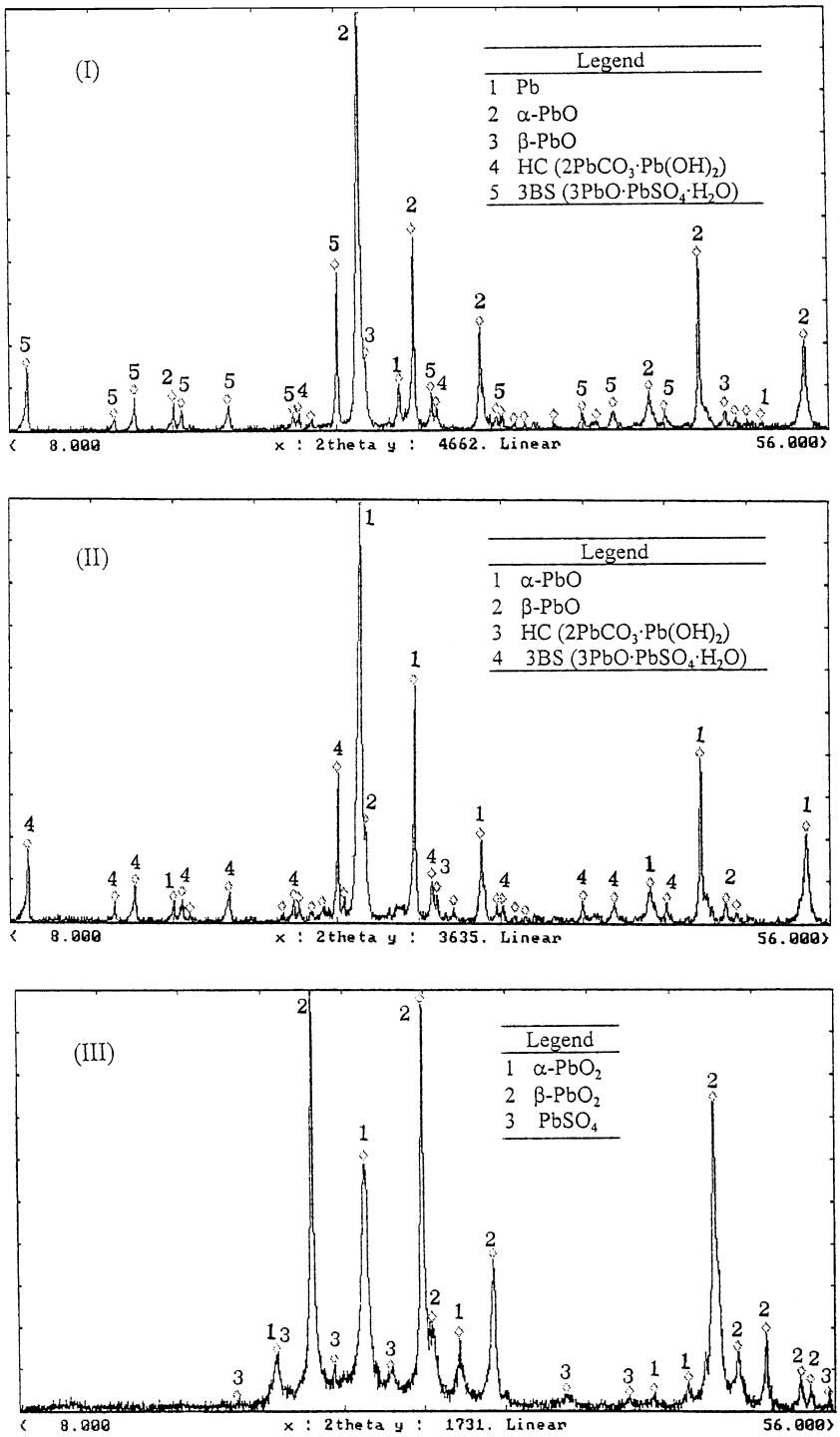

Fig. 1. XRD patterns for samples from group A: (I) pasted plates; (II) cured plates; (III) formed plates.

Table 2 presents the physicochemical and XRD analyses of all sulfates in the pastes, in plates after curing at 50°C, and in plates after formation. The results show that the major paste constituents are α-PbO and tribasic lead sulfate (3BS) together with some lead and β-PbO. During paste mixing, the temperature is maintained below ~50°C and tetra basic lead sulfate (4BS) is not formed in the paste. Some studies of formation [5–8] have shown that 4BS favors the formation of α-PbO_2, and that 3BS yields β-PbO_2. Similar to our former results [6], the data in Table 2 reveals that the β-PbO_2 phase forms proportionately to the 3BS content. The XRD patterns for samples from group A in pasted, cured and formed plates are given in Fig. 1. Table 2 also indicates that sample C produces paste, cured and formed plates with the lowest surface-area. The difference in specific surface-area in all of three samples, however, is small. Since the α-PbO_2 crystals are larger than the β-PbO_2 crystals, the formed group C plates with more α-PbO_2 have the smallest BET specific surface-area. The pore-size distributions for formed pastes at different compositions (groups A–C) are shown in Fig. 2. The results show that the formed A plates have the largest pore-size and cumulative volume. The cumulative volumes of A, B, and C samples are 0.141, 0.12 and 0.10 ml g^{-1}, respectively. Scanning electron micrographs of formed crystals in the groups A–C samples are presented in Fig. 3. The major constituents are α-PbO_2 and β-PbO_2 with some $PbSO_4$ in the formed plate. All of the three formed plates display the typical development of crystalline PbO_2 with each grain consisting of many sub-grains.

3.2. Cell standard cycle-life performance

This work has also attempted to determine the effects of different paste compositions on cell performance. The average performance tested in the 5 cells in each group was based on the results exhibited by these five cells. Table 3 lists the values of the rate of capacity loss and the average capacity delivered per cycle. Both are based on the cell performance before the capacity had fallen to 80% of the rated value (4.0 Ah). The capacity loss rate *Y*, expressed as %/cycle, is based on the initial capacity and is estimated by

$$Y = (1 - C_{+}^{1/n}) \times 100 \quad (1)$$

where n denotes the total cycle number and C_+ represents the terminal fractional capacity (based on the initial cell capacity). According to Table 3, group A plates have a higher initial capacity but a shorter cycle-life and, thereby, a

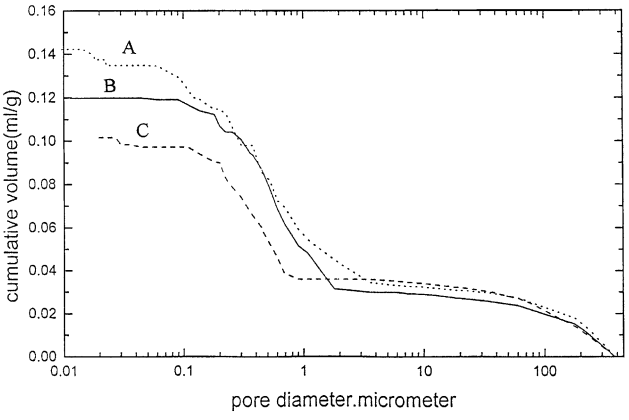

Fig. 2. Pore-size distributions for formed A, B and C plates.

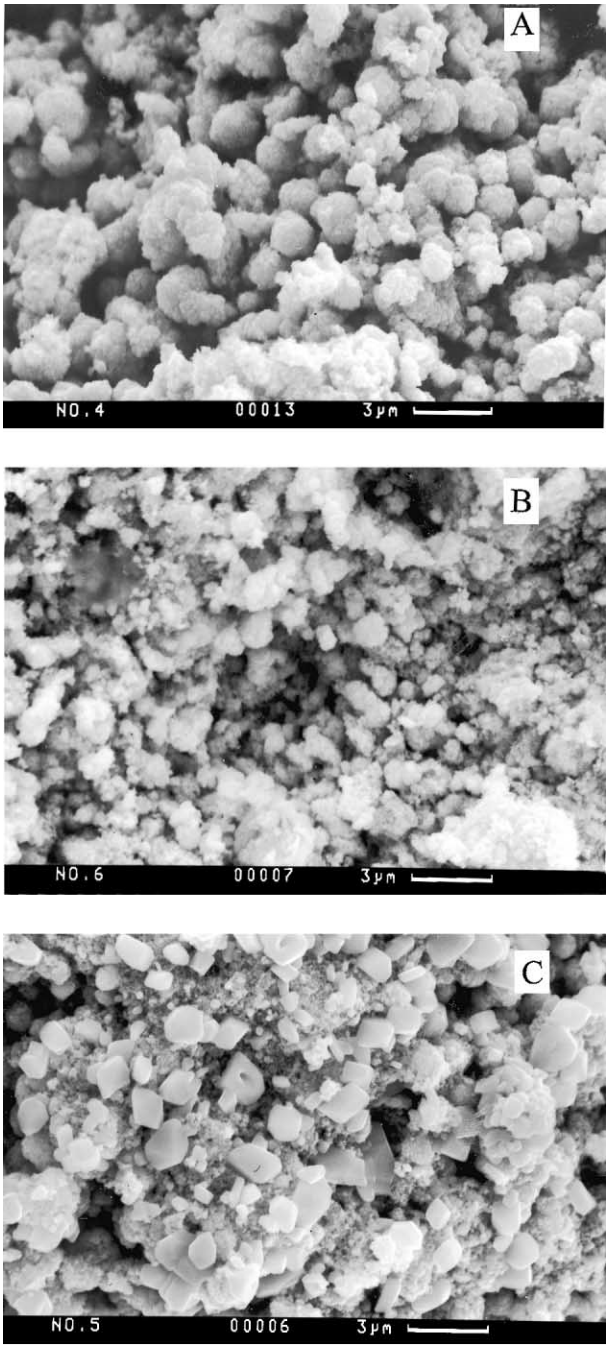

Fig. 3. Scanning electron micrographs of formed crystals in group A, B, and C plates.

Table 3
Cycle-life performance of representative groups of 4.0 Ah VRLA cells

Sample	Cycle number	Initial capacity (Ah)	Capacity loss/cycle (%)	Average capacity/cycle (Ah)
Group A				
A1	174	4.27	0.1658	4.03
A2	170	4.25	0.1668	4.04
A3	168	4.24	0.1673	4.01
A4	172	4.20	0.1581	4.09
A5	160	4.18	0.1680	4.06
Group B				
B1	192	4.23	0.1475	4.04
B2	194	4.20	0.1401	4.02
B3	188	4.18	0.1420	4.08
B4	187	4.24	0.1516	3.97
B5	179	4.21	0.1493	4.05
Group C				
C1	182	4.18	0.1501	3.94
C2	180	4.20	0.1510	4.01
C3	178	4.19	0.1513	3.90
C4	183	4.15	0.1420	3.98
C5	185	4.17	0.1430	4.05

higher capacity loss per cycle. By contrast, group C has the lowest initial capacity. Group B shows the best combined performance in terms of capacity and cycle-life. Thus, pastes with more water (group A) have a greater porosity which causes a higher active material utilization and a higher initial capacity. The plates have, however, too much porosity and this results in poor mechanical strength and a higher capacity loss per cycle. Adding more H_2SO_4 to the paste produces a smaller porosity and lower capacity, but cycle-life is longer. Plots of capacity versus cycle number are given in Fig. 4 for cells A1, B1, and C1. The capacity of all cells reached their maximum value after roughly 20 cycles, and remained above 80% up to 180 cycles at 100% depth-of-discharge (DoD).

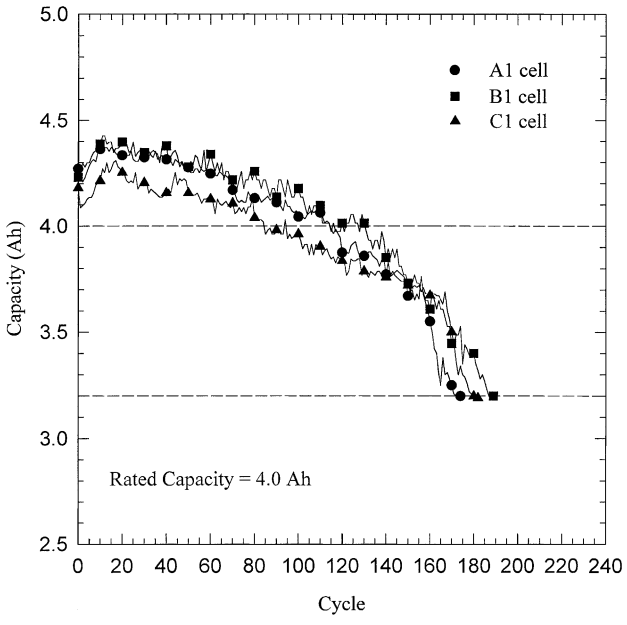

Fig. 4. Capacity vs. cycle number for cells A1, B1 and C1.

3.3. An ac impedance analyses

Impedance measurements were carried out as a function of frequency with Schlumberger 1286 TFA equipment. The contribution of the positive plate was analyzed separately by means of conventional three-electrode wiring. The positive and negative plates were used as the working and counter electrodes, respectively. The reference electrode was a saturated mercurous sulfate electrode and the electrolyte was sulfuric acid solution of 1.26 relative density. The impedance was measured at frequencies between 0.001 and 10 kHz under a desired voltage (E) between working and reference electrodes. Typical Nyquist diagrams obtained at various voltages (E) for group plates A, B, and C are presented in Fig. 5. Group A plates exhibit a high-frequency inductive loop. Many Studies [9–11] have explained that the high-frequency inductive loop lies in the porous structure of the battery electrode and is due to an axial concentration gradient (normal to the electrode surface) in this structure. Hence, the appearance of a high-frequency inductive loop indicates that the group A plates have high levels of porous active materials. This finding is consistent with the BET surface and pore-size analyses and accounts for the larger surface-area, pore-size and initial capacity of the group A cells. Fig. 5 also shows that the smaller voltage, E, with a larger polarization, exhibits a larger charge-transfer resistance, R_{ct}. This result indicates that the smaller E with a higher polarization will reduce the active surface area of PbO_2 and cause an increase in the reaction resistance between PbO_2 and H_2SO_4.

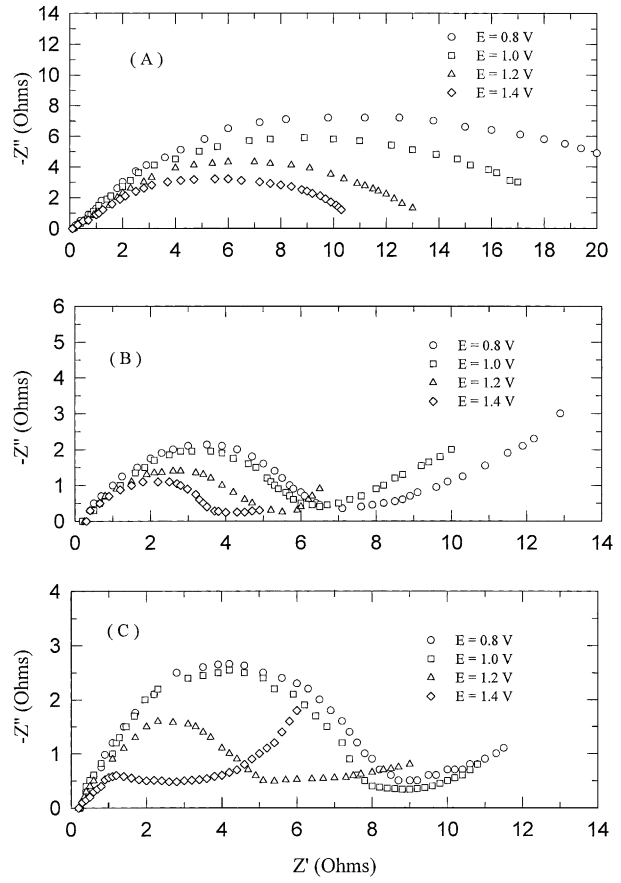

Fig. 5. Nyquist impedance plot at various voltages (E) for group A, B, and C plates.

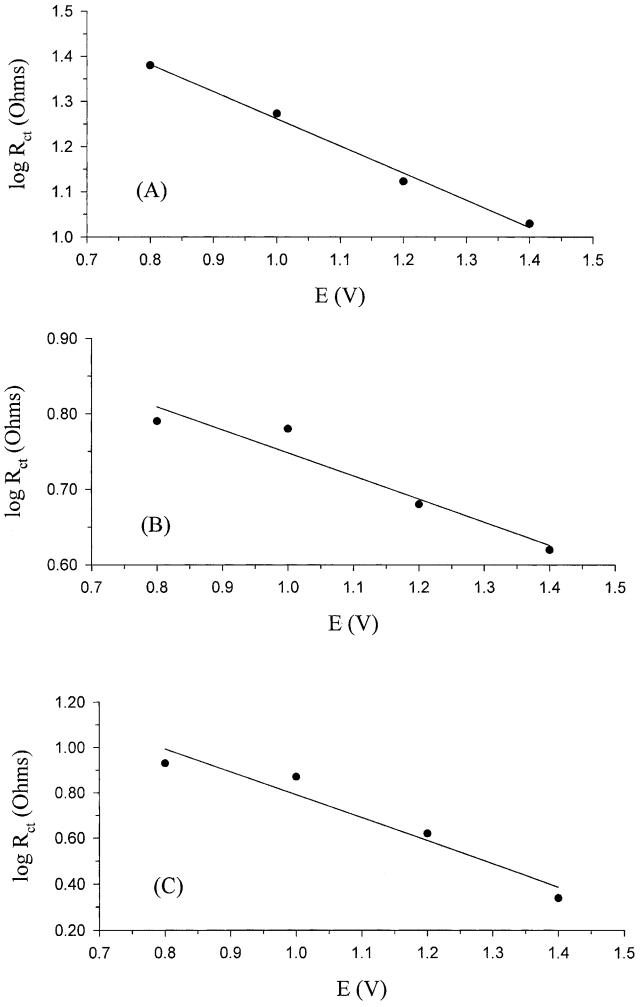

Fig. 6. Log(R_{ct}) vs. E for formed group A, B, and C plates.

Plots of log(R_{ct}) versus E for group plates A, B, and C are shown in Fig. 6. Straight lines were obtained (Fig. 6). The value of R_{ct} at $E_{eq} = 1.442$ V for the equilibrium potential between the working and reference electrodes can be measured from Fig. 6. Values for R_{ct} at the equilibrium potential for the three groups of plates are given in Table 4. According to the charge-transfer resistance equation [12], the exchange current, i_0, can be calculated from

$$i_0 = \frac{RT}{(nFR_{ct})} \tag{2}$$

where R is the gas constant, T the absolute temperature, n the number of moles of electrons transferred, and F is the Faraday constant The calculated values for i_0 for group plates A, B, and C are listed in Table 4. Group C plates exhibit the lowest charge-transfer resistance and the highest exchange current, i_0. Many papers [9,10] have shown that the exchange current of α-PbO_2 is larger than β-PbO_2. Hence, the α-PbO_2 crystals have a higher reaction activity and a lower value for R_{ct}. According to the previous plate composition and morphology analyses, the group C plates contain more α-PbO_2 which causes a smaller charge-transfer resistance and a larger exchange current.

Table 4
Charge-transfer resistance, R_{ct} at $E = 1.442$ V, and exchange current, i_0 data for representative groups

Sample	Charge-transfer resistance (R_{ct} at $E = 1.442$ V)	Exchange current (i_0)
Group A	10	1.27×10^{-3}
Group B	3.9	3.10×10^{-3}
Group C	2.2	5.84×10^{-3}

4. Conclusions

This work has attempted to determine the effects of various $H_2SO_4/H_2O/PbO$ ratios in positive pastes on the material structure and electrochemical characteristics of the resulting plates. The following conclusions can be made:

1. From physicochemical and XRD analyses of all sulfates both in the pastes and in the plates after curing at 50°C

and formation, the results show that the major paste constituents are α-PbO and tribasic lead sulfate (3BS).

2. Sample A has the largest specific surface-area in both pastes and cured/formed plates. The cumulative volumes of A, B, and C samples are 0.141, 0.12 and 0.10 ml g^{-1}, respectively. Sample A has the highest pore-size but a low BET specific surface-area. Sample C has the smallest pore-size and the smallest specific surface-area.
3. Testing has shown that pastes with more water have a greater porosity. This results in high active-material utilization and high initial capacity. On the other hand, plates with too much porosity have poor mechanical strength, which gives rise to a high capacity loss for each cycle. Adding more H_2SO_4 to the paste produces a smaller porosity and a lower capacity, but cycle-life is longer.
4. According to ac impedance measurements, group A plates exhibit a high-frequency inductive loop. The appearance this loop suggests that the plates have active-materials of high porosity during plate preparation. This result is consistent with BET surface and pore-size analyses and gives rise to greater initial capacity. Group C plates contain more α-PbO_2 which causes a smaller charge-transfer resistance and a larger exchange current.

Acknowledgements

The authors thank Ztong Yee Battery Corporation (Taiwan GS) for providing several electrodes and cell parts. The experimental assistance provided by Mr. C.F. Chou and Mr. C.D. Jeng is also gratefully acknowledged.

References

[1] W.R. Kitchens, R.C. Osten, D.W.H. Lambert, J. Power Sources 53 (1995) 263–267.
[2] L.T. Lam, O. Lim, H. Ozgun, D.A.J. Rand, J. Power Sources 48 (1994) 83–111.
[3] B. Culpin, D.A.J. Rand, J. Power Sources 36 (1991) 415–438.
[4] D. Pavlov, E. Bashtavelova, J. Electrochem. Soc. 131 (1984) 1468.
[5] D.A.J. Rand, R.J. Hill, M. McDonagh, J. Power Sources 31 (1990) 203–215.
[6] J.-S. Chen, L.F. Wang, J. Power Sources 70 (1998) 269–273.
[7] L. Zerroual, N. Chelali, F. Tedjar, J. Power Sources 51 (1994) 425–431.
[8] J. Burbank, J. Electrochim. Acta 15 (1970) 1221.
[9] M. Keddam, C. Rakotomavo, H. Takenouti, in: Proceeding of the Symposium on Advanced in Lead-Acid Batteries, Proc. Electrochem. Soc. 84-14, p. 277.
[10] N.A. Hampson, S. Kelly, K. Peters, J. Appl. Electrochem. 11 (1981) 751.
[11] N.A. Hampson, S. Kelly, K. Peters, J. Appl. Electrochem. 11 (1981) 765.
[12] P.H. Rieger, Electrochemistry, 2nd Edition, Chapman & Hall, New York, USA, 1993, p. 326.